

C.P. No. 1162

C.P. No. 1162



ROYAL AIR FORCE ESTABLISHMENT
BEDFORD.

MINISTRY OF AVIATION SUPPLY

AERONAUTICAL RESEARCH COUNCIL

CURRENT PAPERS

Low-Speed Wind-Tunnel Calibrations of the Pitot and Static Pressure Sensors and Wind Vanes on the Short SC I Aircraft

by

K. P. King and E. N. Rowthorn

Aerodynamics Dept., R.A.E., Bedford

LONDON: HER MAJESTY'S STATIONERY OFFICE

1971

PRICE 45p NET

LOW-SPEED WIND-TUNNEL CALIBRATIONS OF THE PITOT AND STATIC PRESSURE
SENSORS AND WIND VANES ON THE SHORT SC 1 AIRCRAFT

by

K. P. King
E. N. Rowthorn

Aerodynamics Dept., RAE, Bedford

SUMMARY

The pressure sensors tested consisted of a perforated sphere static, a twin venturi pitot arrangement, designed to permit the derivation of dynamic pressure in both forward and backward flight, and a Mk.8T pitot-static head. It was found that only the Mk.8T pitot-static head gave satisfactory results over the range of sideslip angles likely to be met in flight. This pitot-static head was then calibrated over a range of incidence and sideslip angles and error contours were plotted to facilitate the correction of the indicated static and dynamic pressures recorded in flight. The wind vanes measuring sideslip and incidence were also calibrated over the same range and error contours plotted for the correction of their indications. Finally the dynamic response of the wind vanes was investigated to determine their natural frequency and damping and hence their amplitude ratio and phase lag when recording aircraft oscillations.

* Replaces RAE Technical Report 70133 - ARC 32780.

CONTENTS

	<u>Page</u>
1 INTRODUCTION	3
2 DESCRIPTION OF SENSORS	4
2.1 The Mk.8T pitot-static head	5
2.2 The perforated sphere static	5
2.3 The venturi pitots	5
2.4 The wind vanes	6
3 TESTS MADE	6
3.1 Preliminary tests	6
3.2 Calibration of the Mk.8T pitot-static head	7
3.3 Calibration of the wind vanes	8
3.3.1 Static calibration	8
3.3.2 Dynamic response tests	8
4 RESULTS AND DISCUSSION	9
4.1 Preliminary tests	9
4.2 Calibration of the Mk.8T pitot-static head	12
4.3 Wind vane static calibration	14
4.4 Wind vane dynamic response	14
4.4.1 Response to incidence produced by aircraft rotary motion	15
4.4.2 Response to incidence produced by aircraft translatory motion	16
5 CONCLUSIONS	16
Acknowledgements	19
Symbols	19
References	20
Illustrations	Figures 1-14
Detachable abstract cards	-

1 INTRODUCTION

The measurement of an aircraft's airspeed and altitude is always difficult since, in general, it is not possible to measure exactly the free stream static and total pressures from which airspeed and altitude are normally derived. This is partly because it is not practical to mount pressure sensors far enough away from the airframe to be outside the aircraft pressure field but also because of the sensitivity of the measured pressures to the changes of incidence and sideslip encountered in flight. Nevertheless the conventional pitot-static head when mounted in a sensible position on the airframe does permit the derivation of airspeed and altitude for conventional aircraft with relatively small errors, except perhaps at high subsonic and transonic Mach numbers^{1,2}.

With jet-lift VTOL aircraft however the problem is more severe for three main reasons. Firstly, VTOL aircraft can fly at much lower speeds than conventional aircraft and ideally it should be possible to measure airspeed accurately down to zero or even negative values. Secondly VTOL aircraft, when partly or fully jet-supported, can fly with much larger incidence and sideslip angles than can be tolerated by conventional aircraft. In fact sideways translation, with a sideslip angle of 90° , is a common manoeuvre for VTOL aircraft when hovering. Thirdly the high velocity jet efflux providing jet lift considerably alters the pressure field that would exist around the aircraft simply as a result of forward motion. This means that the background of experience that has been built up concerning the best position to site the pitot-static head on conventional aircraft may not be sufficient for VTOL aircraft.

The same problems have, of course, existed for a long time with helicopters when flying at low speed but as yet no means of determining airspeed and altitude which is clearly superior to the conventional pitot-static head has been found. For certain specific roles, e.g. anti-submarine warfare, radar is used to determine altitude and ground speed accurately but in general a conventional pitot-static head is relied upon and operational limitations have to be imposed as a result of the inaccuracies in the indications at low speed.

Since the Short SC 1 is a research aircraft which was built specifically to explore the partly jet-borne regime it is required to record static and dynamic pressures for the determination of altitude and airspeed (at least down to zero forward speed) as accurately as possible for flight test purposes. The accuracy required depends very much on the type of test being undertaken and in some cases it is pressure changes that are required accurately rather than absolute pressures but, as a rough guide, the order of accuracy required for

airspeed is $\pm\frac{1}{2}$ kt from 200 kt to zero (or ideally to -20 kt) and for altitude ± 10 ft from zero to 10000 ft. For this reason, as well as a conventional pitot-static head to supply the pilot's instruments, three more pressure sensors, a perforated sphere static and two venturi pitots were provided on the aircraft to supply the required pressures to the test instrumentation. The perforated sphere static was expected to be an improvement over the conventional static sensors at large angles of incidence and sideslip while the two venturi pitots represented an attempt to obtain dynamic pressure for the derivation of airspeed in both forward and backward flight. In view of the experimental nature of these sensors it was considered advisable to test their performance in a wind-tunnel, following which the complete noseboom from the aircraft was mounted in the wind-tunnel to calibrate the sensors over the required range of incidence and sideslip angles.

The angles of incidence and sideslip experienced in flight are measured by wind vanes, as is usual on research aircraft. These vanes are subject both to static errors due to interference from the flow fields of their mounting and of the aircraft and to dynamic errors as a result of their inherent response characteristics. Calibrations to determine these errors were therefore carried out at the same time as the calibration of the pressure sensors. The desired accuracy of determination of incidence and sideslip is $\pm 0.1^\circ$ over a range of incidence from -5° to $+25^\circ$ and sideslip from -20° to $+20^\circ$.

In the tests described in this paper the effects of the aircraft's pressure and flow fields and the jet efflux could not, of course, be taken into account. Flight tests to determine the errors due to these effects have also been performed but wind-tunnel tests over a range of incidence and sideslip are necessary for the adequate interpretation of flight test data.

2 DESCRIPTION OF SENSORS

When the SC 1 was built the following pressure and flow direction sensors were incorporated:

- (i) a Mk.8T pitot-static head
- (ii) a perforated sphere static
- (iii) two venturi pitots, one facing forward and one facing aft
- (iv) two wind vanes, one for incidence and one for sideslip.

The pitot-static head, the perforated sphere static, one of the venturi pitots and the wind vanes were mounted on a noseboom while the second venturi pitot was mounted facing aft on the top of the fin. In Fig.1 the positions of the sensors on the noseboom and the venturi pitot on the fin can be seen, while Fig.2 shows the arrangement on the end of the noseboom in more detail.

2.1 The Mk.8T pitot-static head

This unit is of conventional construction having a cylindrical body 6 in (152 mm) long and a hemispherical head. The static pressure sensor is in the form of six circumferential slots arranged in two groups of three, the first group being 3 in (76 mm) from the nose of the unit and the second group $\frac{1}{2}$ in (3.2 mm) behind the first. Each group is symmetrically disposed about the longitudinal axis of the unit and the second is rotated through 60° relative to the first. Since each slot occupies about one-sixth of the tube circumference the complete periphery of the tube is covered by the two groups. Inside the head there is a drain hole $\frac{1}{32}$ in (0.79 mm) in diameter between the pitot and static chambers. Its purpose is to prevent any water collected in the pitot tube from blocking the pitot line or reaching the instruments.

2.2 The perforated sphere static

This unit consists of a tube with a blanked-off end and with sixteen holes of 0.05 in (1.27 mm) diameter drilled as shown in Fig.3. The end of the tube containing the holes is completely enveloped by a sphere whose entire surface apart from the area immediately in front of the blanked-off end of the tube is perforated by 0.1 in (2.54 mm) diameter holes at 0.25 in (6.35 mm) pitch. A table tennis ball was used for this sphere and hence the device came to be known as the 'ping-pong' static or simply p.p. static. This name will be used in the remainder of this Report for the sake of brevity.

The origin of this type of device is not known but the object is to maintain a constant pressure within the sphere regardless of the direction of the flow relative to the axis of the tube, thus making a static sensor free from directional effects. It was intended that this device should supply static pressure to the data recorder to enable altitude to be calculated.

2.3 The venturi pitots

These consist of small pitot tubes mounted inside venturis turned from aluminium. Fig.4 shows the construction and dimensions of the units used. The purpose of mounting the pitot tubes inside venturis in this way is to reduce their sensitivity to flow direction³.

Two venturi pitots were used in an attempt to derive dynamic pressure and hence airspeed for the data recorder in both forward and backward flight. One was mounted on the noseboom (Fig.2) with the pitot facing forward while the second was mounted on the top of the fin with the pitot facing aft. It was

intended that the latter would form a static pressure sensor in forward flight which together with the former would enable airspeed to be derived in the usual way, while in backward flight the roles of the two venturi pitots would be reversed.

2.4 The wind vanes

The wind vanes in use at the time of the initial tests on the pressure sensors were not very satisfactory mainly because of excessive friction and hysteresis and before the final calibrations were commenced they were replaced by a model that had been designed in the Aero Flight Division at R.A.E. Bedford. In this model special attention had been paid to low speed performance by increasing the vanes' aerodynamic stiffness and also reducing friction and hysteresis by using variable reluctance transducers mounted directly onto the vane shaft. This arrangement resulted in a slightly larger diameter mounting boom which had a small effect on the static error of the Mk.8T pitot-static head. This is mentioned in section 4.2. The vanes can clearly be seen in Fig.2 while a drawing showing the pertinent dimensions of the vane assembly is shown in Fig.5.

3 TESTS MADE

Since the sensors provided for supplying static and dynamic pressures to the data recorder were somewhat unconventional it was considered advisable to test their performance over a range of sideslip angles in a wind-tunnel. The object of these preliminary tests was simply to establish whether or not they would give satisfactory results and whether they were in fact any better than the Mk.8T pitot-static head. Following these tests the Mk.8T pitot-static head and the wind vanes were calibrated over the required ranges of incidence and sideslip. All the tests were made in the 13ft x 9ft (4 m x 3 m) wind-tunnel at R.A.E. Bedford.

3.1 Preliminary tests

The sensors intended to provide dynamic pressure for the determination of airspeed were the two venturi pitots. To evaluate this novel idea for obtaining airspeed in both forward and backward flight, they were mounted, facing in opposite directions, on a boom which could be rotated allowing them to be yawed through 360° without any interference from the boom. The pressures sensed by each were then measured over a range of 240° .

The next step was to test the p.p. static but since the one shown in Fig.2 was an integral part of the noseboom a new pipe was made to the dimensions shown in Fig.3. The perforated sphere was then removed from the device on the noseboom and attached to the new pipe. The p.p. static thus made was mounted in place of one of the venturi pitots on the boom in the wind tunnel and tested over a range of $\pm 45^\circ$.

The perforated sphere was subsequently replaced on the noseboom and, as soon as it became convenient, the complete noseboom was removed from the aircraft and mounted in the wind-tunnel in such a way that it would be rotated in both pitch and yaw. Tests were first made to compare the performance of the venturi pitot and p.p. static with that of the Mk.8T pitot-static head in conditions which, apart from the absence of the aircraft, were representative of flight, where it was thought that the various devices on the end of the noseboom might significantly interfere with one another, particularly at large angles of incidence and/or sideslip.

As soon as the first results were obtained it became apparent that the p.p. static and venturi pitot when mounted on the noseboom did not give satisfactory results. Consequently only the MK.8T pitot-static head was fully calibrated.

3.2 Calibration of Mk.8T pitot-static head

The variation with speed of the error in the indicated static and total pressures was first investigated in order to choose a suitable speed for the calibration and to verify that a calibration performed at one speed would be valid over the speed range of interest. This test was first made with the head aligned with the flow and then at a number of angles of sideslip in the range $\pm 20^\circ$. Finally a check was made at the extreme angle to the total flow direction of $35\frac{1}{2}^\circ$ which was achieved by setting $\alpha = 20^\circ$ and $\beta = 30^\circ$ where α and β are the angles of incidence and sideslip and are defined by:

$$\alpha = \tan^{-1} \frac{w}{u} \quad (1)$$

$$\beta = \sin^{-1} \frac{v}{V} \quad (2)$$

where u = component of free stream velocity parallel to noseboom x-axis
 v = component of free stream velocity parallel to noseboom y-axis
 V = free stream velocity
 w = component of free stream velocity parallel to noseboom z-axis.

After this a speed of 200 ft/s (61 m/s) was selected and the calibration performed over a range of incidence from -5° to $+25^{\circ}$ and a range of sideslip from -20° to $+20^{\circ}$.

3.3 Calibration of the wind vanes

Wind vanes are subject both to static errors, which are continually present since they arise from the flow field around any objects near to the vanes, and to dynamic errors which occur when incidence or sideslip are changing sufficiently rapidly for the response of the vane to be inadequate. It is thus necessary to perform both a static calibration and a dynamic response test in order to be able to correct any instantaneous indicated value of incidence or sideslip to the true value.

3.3.1 Static calibration

As previously mentioned the purpose of this calibration was simply to find the effect of the wind vane mounting and of any other objects on the noseboom that were near enough to affect the vanes. The effects of the aircraft's flow field and jet efflux could not, of course, be taken into account.

This test was conducted simultaneously with the calibration of the pitot-static head and so covered a range of incidence from -5° to $+25^{\circ}$ and a range of sideslip from -20° to $+20^{\circ}$.

3.3.2 Dynamic response tests

Wind vanes possess inertia and are subject to forces giving rise to stiffness and damping. If one ignores the small parasitic torque from the electrical pick-off, which is negligible compared with any of the other forces acting on the vanes, the stiffness is entirely due to aerodynamic forces while the damping is due to both aerodynamic and internal viscous forces. The relative contributions are discussed in section 4.4. Wind vanes are thus essentially second order systems and when flow angles are changing rapidly, such as when the aircraft is performing pitch oscillations or dutch rolls, the vane amplitude may not be the same as that of the forcing function and may not be in phase with it. It is therefore important to know the relationship between the vane oscillation and the aircraft oscillation, i.e. the vane's amplitude ratio and phase lag. To determine these for any given conditions it is first necessary to know the vane's natural frequency and damping ratio and to find these, vane oscillations were recorded at a number of wind speeds.

Since both wind vanes were identical the tests were performed on the side-slip vane only. To start the vane oscillating, a rod was passed through a hole in the top of the tunnel working section into a support just behind the vane. A finger was attached to the rod in such a position that when the rod was rotated the finger deflected the vane and then released it suddenly. This test was performed at speeds of 50, 100, 150, 200 and 250 ft/s (15, 30, 46, 61 and 76 m/s) and the vane output was recorded on the data recorder that is used in the aircraft.

4 RESULTS AND DISCUSSION

4.1 Preliminary tests

The idea of using two opposite-facing venturi pitots to obtain dynamic pressure for the determination of airspeed, though interesting in principle, proved to be impractical. The pressures that each indicated when yawed through 240° are shown in Fig.6 in the form of pressure coefficients where C_{PR} is the coefficient of indicated pressure and is defined as:

$$C_{PR} = \frac{R - p_w}{q}$$

where R = indicated pressure

p_w = working section static pressure

q = free stream kinetic pressure.

It can be seen that when facing upstream total pressure was accurately measured at inclinations up to about 30° to the flow direction but when facing downstream the variation of the indicated pressure with sideslip angle was rather erratic. Because of this irregular variation even over the comparatively small range required for measurements in flight (i.e. $\pm 20^\circ$) it was decided that this was not a practical system for obtaining dynamic pressure. This result is hardly surprising, in view of the use of an aft-facing venturi pitot as a static pressure sensor, but since the system had been provided on the aircraft it was considered that it should at least be tested.

The p.p. static, which was tested next, showed great promise of being a good static pressure sensor over a wide range of sideslip angles. Fig.7 shows the pressure that it indicated, plotted as C_{PR} , against sideslip angle.

Although the pressure indicated was somewhat less than true static pressure it varied very little over the range $\pm 45^\circ$.

The second venturi pitot was left in position on the boom so that while the p.p. static was being tested the pressure indicated by the venturi pitot could be recorded in smaller steps to define more precisely the sideslip range over which it is accurate. These results are also shown in Fig.7 and it can be seen that this particular device is slightly asymmetric. This could be due to a slight irregularity in either the venturi or pitot entry, or failure to position the pitot tube exactly in the centre of the venturi for any of these factors can affect the range over which total pressure is faithfully recorded⁴.

The results of the foregoing tests indicated that the venturi pitot and p.p. static should be satisfactory pressure sensors for providing static and dynamic pressures for data recording, but to check their performance when mounted on the aircraft noseboom and to compare them with the Mk.8T pitot-static head further tests were undertaken as described in section 3.1. The results of these tests are shown in Figs.8 and 9 which show respectively the variation of static pressure with sideslip angle for the p.p. static and Mk.8T pitot-static head and the variation of dynamic pressure with sideslip angle for the venturi pitot/p.p. static combination and the Mk.8T pitot-static head.

From Fig.8, which shows the static pressure in the form of the coefficient C_{pR} , it can be seen that the performance of the p.p. static on the noseboom was significantly worse than that of the one tested previously. The variation in the indicated pressure was nearly 4 times greater than in the previous tests and, as well as being asymmetric about the zero sideslip position, it was rather erratic. The dynamic pressures are shown in Fig.9 as the ratio of the measured dynamic pressure to the free stream kinetic pressure, i.e.

$$\frac{H - p}{q}$$

where H = measured total pressure
 p = measured static pressure
 q = free stream kinetic pressure.

It can be seen that the dynamic pressure obtained from the venturi pitot/p.p. static combination is decidedly asymmetric and irregular. Within the range $\pm 30^\circ$ where the performance of the venturi pitot is very good the irregularity

is obviously due to the p.p. static but outside this range the venturi pitot also is asymmetric and is contributing to the asymmetry in the indicated dynamic pressure.

The disappointing behaviour of the p.p. static on the aircraft noseboom is thought to be due partly to interference from the Mk.8T pitot-static head and the wind vane assembly and partly to a slight misalignment that was discovered later between the perforated sphere and the pipe on which it is mounted. Earlier unpublished work at R.A.E. had shown that the performance of such devices was rather sensitive to a number of factors, e.g. size of sphere, size and spacing of perforations, position of static sensor within sphere, etc. Although it is felt that the device does have the potential for development into a useful static pressure sensor it was not possible at the time of these tests to undertake the necessary development. Neither was it considered worth spending time trying to modify the noseboom to reduce interference effects. Consequently it was decided to use the Mk.8T pitot-static head to supply static and dynamic pressures to the data recorder as well as to the pilot's instruments. Although there are large errors in the static and total pressures indicated by this device at the maximum sideslip angle required ($\pm 20^\circ$), the indicated pressures do vary in a regular fashion with sideslip and are much more nearly symmetrical about the zero sideslip position than with the venturi pitot/p.p. static combination. There is nevertheless a slight asymmetry in the pressures indicated by the pitot-static head. A close examination of the head revealed that the plane containing the pitot entry was possibly not exactly normal to the axis of the head and that some of the static slots had burrs or small particles of dirt adhering to their edges. Both of these defects have been shown to cause asymmetric errors^{5,6} as has non-uniformity in the size of the static slots and asymmetry in the space inside the head near the static slots. These defects therefore may well be contributing to the asymmetry in the indicated pressures although interference from the other devices on the noseboom is undoubtedly a significant factor.

A further possible advantage stemming from the use of the Mk.8T pitot-static head for recording purposes is that the airspeed and altitude derived directly from the recorded data should be the same as those displayed to the pilot. At the time of writing this had already been of value in showing up an ASI instrument error.

4.2 Calibration of the Mk.8T pitot-static head

The purpose of the calibration is, of course, to find the errors in the indicated pressures over the sideslip and incidence range of interest but, as described in section 3.2, a check was first made on the variation of the errors with speed. The results of this are shown in Fig.10 where the total and static pressure errors are plotted as coefficients C_{P_H} and C_{P_P}

$$C_{P_H} = \frac{\Delta H}{q} = \frac{H - H_o}{q}$$

and

$$C_{P_P} = \frac{\Delta p}{q} = \frac{p - p_o}{q}$$

where H = measured total pressure

H_o = free stream total pressure

p = measured static pressure

p_o = free stream static pressure.

ΔH , Δp and q were calculated from measurements of the working section static pressure and settling chamber pressure and the tunnel calibration factors.

When the pitot-static head is aligned with the flow direction (Fig.10a) the errors are small and are constant down to almost 100 ft/s (30 m/s). The increase in static error over that shown in Fig.8 is believed to be due to increased interference from the larger mounting boom of the new wind vane assembly fitted at the time of this test. When the pitot-static head is yawed through 20° (in such a way that the p.p. static is downstream to minimise the effect of interference from this device) the errors are larger (Fig.10b) but the variation with speed is no greater; in fact the variation of pitot error has disappeared. No explanation for this has been found but it is believed that at $\beta = 0$ the increase in error below about 100 ft/s (30 m/s) may be due to the effect of Reynolds number on the flow through the drain hole between the pitot and static chambers. Tests on a Mk.9A pitot-static head⁷, which also has a drain hole between the pitot and static chambers, revealed that the drain hole was responsible for a significant error in static pressure and there was evidence that suggested that the variation of this error with speed was due to the effect of Reynolds number on the flow through the drain hole.

Fig.10c shows the errors when the pitot-static head is inclined at 35.5° ; this angle being achieved by yawing through 30° and pitching through 20° . Such a large angle is well beyond the range over which it is intended to use the pitot-static head, but it was considered worth showing the result to illustrate how the head behaves at such an extreme angle. The variation of the errors with speed is almost certainly due to Reynolds number effects. However it cannot be attributed to a change in the crossflow conditions from subcritical to supercritical for at the highest speed tested (200 ft/s) (61 m/s) the crossflow Reynolds number was 0.54×10^5 and this is well below the critical value for a cylinder inclined at that angle as determined by Bursnall and Loftin⁸. Nevertheless Ref.8 shows that even when the flow remains subcritical the pressure distribution over the rear half of an inclined cylinder does vary with Reynolds number because this parameter affects the character of the wake behind the cylinder, and so the pressure sensed by the static slots which encircle the head can be expected to vary.

Another factor is the effect of Reynolds number on the possible vortex formation at the nose of the pitot-static head. This is likely to significantly affect the pressure distribution at the position of the static slots which are only 3.5 diameters from the nose.

After these checks on the effect of speed the pitot-static head was calibrated as described in section 3.2. The results are shown in Fig.11 in the form of contours of the static pressure coefficient C_{pp} (Fig.11a) and the dynamic pressure error (Fig.11b) expressed as the coefficient

$$C_{pD} = \frac{(H - p) - (H_0 - P_0)}{q} .$$

This method of presentation was chosen to facilitate the correction of the static and dynamic pressures recorded in flight.

Tests on a Mk.8A and a Mk.8B pitot-static head, which only differ from each other and from the Mk.8T head in the type of heating element used, are reported in Ref.9. It should be noted, however, that the tests reported in Ref.9 were made with the drain hole between pitot and static chambers sealed. No direct comparison with these results is possible, since the lowest speed at which tests were made was $M = 0.4$, but the results of the tests at this Mach number up to inclinations of 20° are in reasonable agreement with the results presented here of the tests at 200 ft/s (61 m/s) (i.e. $M \approx 0.2$). It is also interesting to note that at all the Mach numbers tested in Ref.9 the variation of dynamic pressure with incidence between 0 and 20° follows the same pattern as shown in Fig.9.

4.3 Wind vane static calibration

In order to determine the errors in the wind vane readings it is important to define the angles that they are supposed to measure since there is a choice of definitions of both incidence and sideslip. The angles that were set in the wind-tunnel, which are defined by equations (1) and (2) in section 3.2, are, of course, determined by the method of suspending and rotating the noseboom in pitch and yaw and it is fortuitous that the same definitions of incidence and sideslip are customarily used in flight mechanics. However, if the wind vanes aligned themselves perfectly with the component of airflow in their own plane of movement, while the incidence vane would record the angle defined by equation (1) the sideslip vane would record an angle defined by:

$$\beta = \tan^{-1} \frac{v}{u} . \quad (3)$$

It is thus convenient to define the wind vane errors not as the difference between what was actually recorded and what a perfect wind vane would record, but as the difference between what was actually recorded and what was set in the wind-tunnel. This has the effect of making the sideslip vane error appear large for large sideslip angles because included in it is the conversion from the angle that a perfect wind vane would measure to the angle that is required for the analysis of flight test results.

The results of the static calibration, which are shown in Fig.12, were plotted as error correction contours to facilitate correction of the indicated values of incidence and sideslip.

4.4 Wind vane dynamic response

The records of wind vane oscillations were analysed to determine the vane's natural frequency and damping and these are shown as functions of airspeed in Figs.13 and 14. The wind vanes had no internal damping deliberately applied, but oil in bearings does give rise to viscous damping and so it can be assumed that a small amount is inevitably present. The damping ratio measured, therefore, is the sum of that due to the aerodynamic damping and that due to internal viscous damping. In a theoretical analysis of the static and dynamic response properties of wind vanes, Pinsker¹⁰ has shown that the aerodynamic damping, when expressed as a damping ratio, does not vary with airspeed whereas the relative internal viscous damping varies inversely with airspeed. It was found by inspection of

Fig.14 that if the aerodynamic contribution, ζ_a , to the total damping ratio was assumed to be 0.047 (as shown by the dotted line) the remainder does vary approximately inversely with airspeed and it was assumed that this was internal viscous damping, ζ_i . The fact that it is not exactly an inverse relationship is probably due to coulomb friction in the bearings which produces a constant damping torque and means that the internal damping is not truly viscous.

As stated above the wind vanes had no internal damping deliberately applied (as is sometimes the case) and so an attempt was made to verify that the part of the damping ratio which varies approximately inversely with airspeed could be accounted for by unintentional internal damping. It was calculated that a damping torque of 0.04 oz in (282 μ Nm) per unit angular velocity (rad/s) was all that was required to account for the damping ratio but an attempt made to measure this did not give repeatable results. Since it was not difficult to believe that such a small damping torque could be present it was not considered worth spending time on more elaborate methods of measurement.

In Ref.10 it is shown that the dynamic response of wind vanes to incidence produced by aircraft rotary motion is quite different from their response to incidence produced by aircraft translatory motion or by gusts and the two cases are therefore treated separately. Expressions for amplitude ratio and phase lag are given for each case and from these and the measured values of natural frequency and damping ratio the response properties of the SC 1 wind vanes have been determined. Since the purpose of the wind vanes on the SC 1 is to record aircraft motion and not gusts, frequencies up to 0.5 c/s (Hz) only need be considered and this allows considerable simplification of the expressions in Ref.10.

4.4.1 Response to incidence produced by aircraft rotary motion

For frequencies up to 0.5 c/s (Hz) since ζ_i and ζ_a are both small the expressions given in Ref.10 for amplitude ratio and phase lag may, with negligible error, be approximated by:

$$|A| \approx 1.0 \quad (4)$$

$$\varepsilon \approx 2\zeta_i \left(\frac{\omega}{\omega_n} \right) \text{ radians} \quad (5)$$

where ω = frequency of aircraft oscillation
 ω_n = wind vane undamped natural frequency

The largest phase lag will occur at low airspeed when the internal damping ratio is at its largest and the wind vane natural frequency is low. Even in the worst condition, however, the phase lag is small as an example will show. At 50 ft/s (15 m/s), $\zeta_i = 0.05$ and an oscillation at 0.5 c/s (Hz) would result in a phase lag of 0.8° .

4.4.2 Response to incidence produced by aircraft translatory motion

As in the previous section the frequency range to be considered and the small damping ratios allow the expressions given in Ref.10 for amplitude ratio and phase lag to be approximated by:

$$|A| \approx 1 + \left(\frac{\omega}{\omega_n}\right)^2 \quad (6)$$

$$\epsilon \approx 2 (\zeta_a + \zeta_i) \left(\frac{\omega}{\omega_n}\right) \text{ radians} \quad (7)$$

In this case the amplitude of wind vane oscillations will always be greater than that of the aircraft oscillations and the difference will increase as airspeed (and hence wind vane natural frequency) is reduced or aircraft oscillation frequency is increased. However, an oscillation at 0.5 c/s (Hz) at 50 ft/s (15 m/s) would be recorded with an amplitude ratio of only 1.02.

The phase lag in this case will also be larger than in the former case since it is proportional to the total damping ratio instead of just the internal damping ratio. At 50 ft/s (15 m/s) an oscillation at 0.5 c/s (Hz) would result in a phase lag of 1.7° but this can be regarded as a worst case and the phase lag will decrease as airspeed increases and/or aircraft oscillation frequency decreases.

5 CONCLUSIONS

The perforated sphere static and two venturi pitots provided on the Short SC 1 for sensing static and total pressures for flight test recording were tested in a low speed wind tunnel. The sensors were initially tested in isolation to evaluate their individual performance and then they were replaced on the aircraft noseboom on which was also mounted a Mk.8T pitot-static head for supplying the required pressures to the pilot's instruments and wind vanes for measuring incidence and sideslip angles. The complete noseboom was then mounted in the wind-tunnel to test the behaviour of all the pressure sensors and the wind vanes in their normal positions.

The initial tests on the twin venturi pitot arrangement which was intended to supply dynamic pressure to the flight recorders in both forward and backward flight showed that this was not a satisfactory method of obtaining dynamic pressure. The results obtained with the first p.p. static tested appeared very promising, but when the device was tested on the aircraft noseboom, its performance was disappointing, probably as a result of inaccurate alignment and interference from the other devices on the noseboom.

Consequently the idea of using the p.p. static and a venturi pitot for measuring dynamic pressure was rejected. Nevertheless it is believed that the perforated sphere static does have the potential for development into a very good omnidirectional static pressure sensor. Such development could not be undertaken at the time of these tests, however, and it was decided to use the Mk.8T pitot-static head as the sensor for the static and total pressures required for flight test recording. This device was then calibrated over the required range of incidence and sideslip angles and error contours were produced to facilitate the correction of indicated pressures.

Within the range of incidence and sideslip over which the head will be used the pressure errors were found not to vary with speed between 300 ft/s (91 m/s) and 100 ft/s (30 m/s). The increase in the errors as speed was further reduced is believed to be due to Reynolds number effects on the flow through the drain hole between the pitot and static chambers. A check outside the required range of incidence and sideslip, with the head inclined at 35.5° to the flow direction, gave results which showed a marked variation of the errors with speed. This is believed to be due to Reynolds number effects on the crossflow, the velocity of which, at such a large angle of inclination, is a significant proportion of the free stream velocity.

Error contours were also produced for the wind vanes and their dynamic behaviour was investigated. It was found that over the range of frequencies likely to be encountered in flight they will faithfully record the amplitude of aircraft rotary oscillations and their phase lag when recording such oscillations may be calculated from a simple formula. When recording aircraft translatory oscillations the wind vanes will slightly exaggerate the amplitude of the motion but their amplitude ratio and phase lag may be calculated from simple formulae.

The way in which the pressure sensors and wind vanes are mounted and the resulting interference between the devices is obviously responsible for some of

the deficiencies in their performance and other users of such devices would do well to pay particular attention to the mounting arrangement to try and reduce interference effects. However in any arrangement where a number of devices are mounted on a single boom it is unlikely that interference could be completely eliminated and these tests have demonstrated the necessity of using the complete boom to obtain representative calibrations.

Flight tests to establish the pressure errors of the Mk.8T pitot-static head in flight have been completed at the time of writing and will be the subject of a further report.

Acknowledgements

The authors wish to thank the staff of the 13ft x 9ft (4m x 3m) wind-tunnel for their assistance in setting-up the experiment and running the wind-tunnel.

SYMBOLS

$ A $	wind vane amplitude ratio
C_{p_D}	$= \frac{(H - p) - (H_o - p_o)}{q}$ coefficient of dynamic pressure
C_{p_H}	$= \frac{H - H_o}{q}$ coefficient of total pressure
C_{p_p}	$= \frac{p - p_o}{q}$ coefficient of static pressure
C_{p_R}	$= \frac{R - p_w}{q}$ coefficient of indicated pressure
H	measured total pressure
H_o	free stream total pressure
p	measured static pressure
p_o	free stream static pressure
p_w	working section static pressure
q	$= \frac{1}{2} \rho V^2$ free stream kinetic pressure
R	indicated pressure
u	component of free stream velocity parallel to body x-axis
v	component of free stream velocity parallel to body y-axis
V	free stream velocity
w	component of free stream velocity parallel to body z-axis
α	angle of incidence
α_i	indicated angle of incidence
β	angle of sideslip
β_i	indicated angle of sideslip
ϵ	wind vane phase lag
ζ	wind vane total damping ratio
ζ_a	wind vane aerodynamic damping ratio
ζ_i	wind vane internal damping ratio
ω	disturbance frequency
ω_n	wind vane undamped natural frequency

REFERENCES

<u>No.</u>	<u>Author</u>	<u>Title, etc.</u>
1	W. Gracey	Measurement of static pressure on aircraft. NACA Report 1364 (1958)
2	W. Gracey	Wind-tunnel investigation of a number of total-pressure tubes at high angles of attack. Subsonic, transonic and supersonic speeds. NACA Report 1303 (1957)
3	G. Kiel	Total-head meter with small sensitivity to yaw. NACA TM 775 (1935)
4	W.R. Russel W. Gracey W. Letko P.G. Fournier	Wind-tunnel investigation of six shielded total-pressure tubes at high angles of attack. Subsonic speeds. NACA TN 2530 (1951)
5	E.W.E. Rogers	The effects of incidence on two Mark 9A pitot-static heads at subsonic speeds. A.R.C.18489 (1956)
6	K. Merriam E.R. Spaulding	Comparative tests of pitot-static tubes. NACA TN 546 (A.R.C.2409) (1935)
7	D.G. Mabey	The calibration at transonic speeds of a Mk.9A pitot-static head with and without flow through the static slots. A.R.C. C.P. 384 (1957)
8	W.J. Bursnall L.K. Loftin Jr.	Experimental investigation of the pressure distribution about a yawed circular cylinder in the critical Reynolds number range. NACA TN 2463 (1951)
9	E.W.E. Rogers C.J. Berry	Tests on the effect of incidence on some pressure heads at high subsonic speeds. A.R.C. C.P. 41 (1950)
10	W.J.G. Pinsker	The static and dynamic response properties of incidence vanes with aerodynamic and internal viscous damping. A.R.C. C.P. 652 (1962)



Fig.1. The S.C.I. hovering

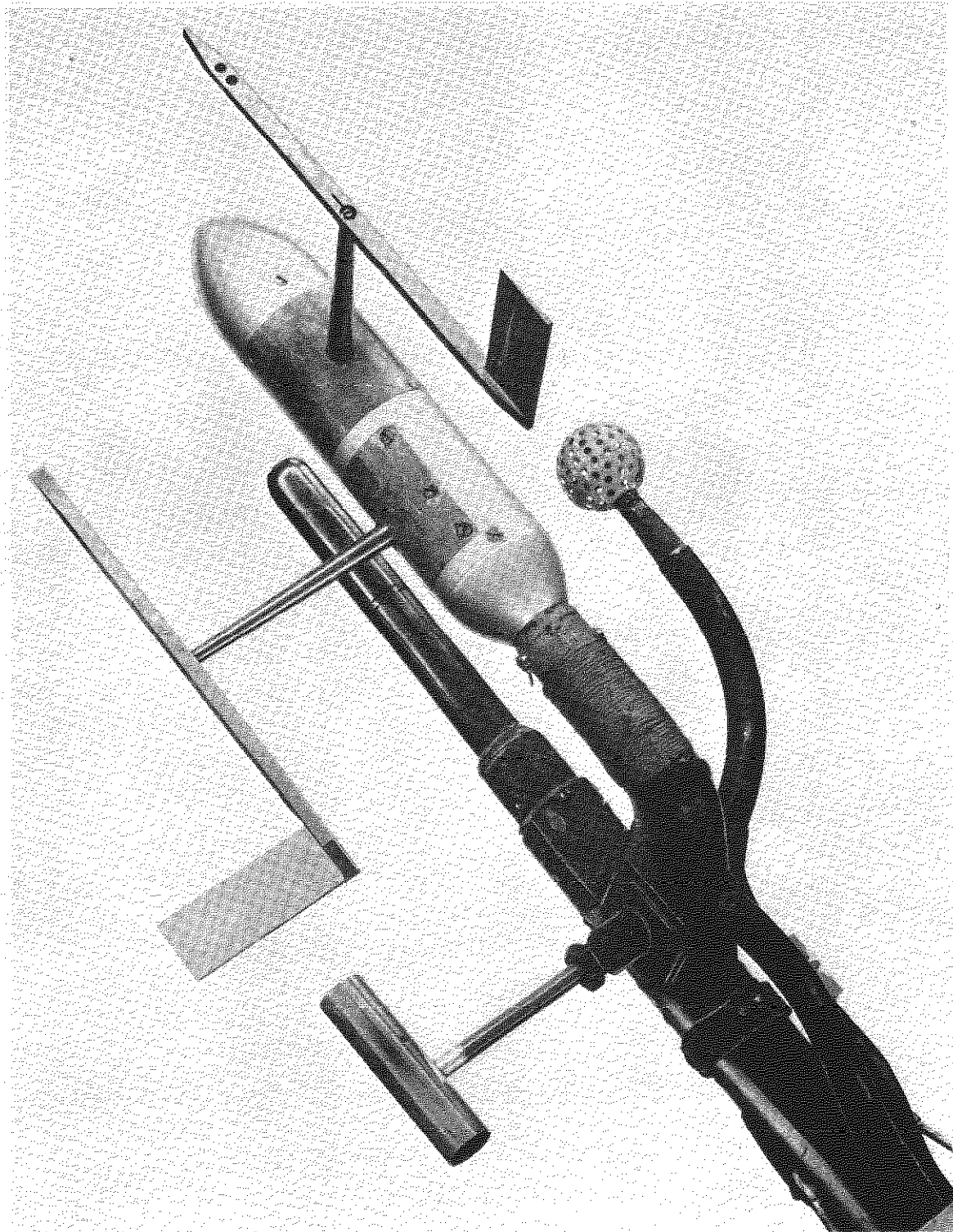


Fig.2. The pressure sensors and wind vanes on the S.C.1. nose boom

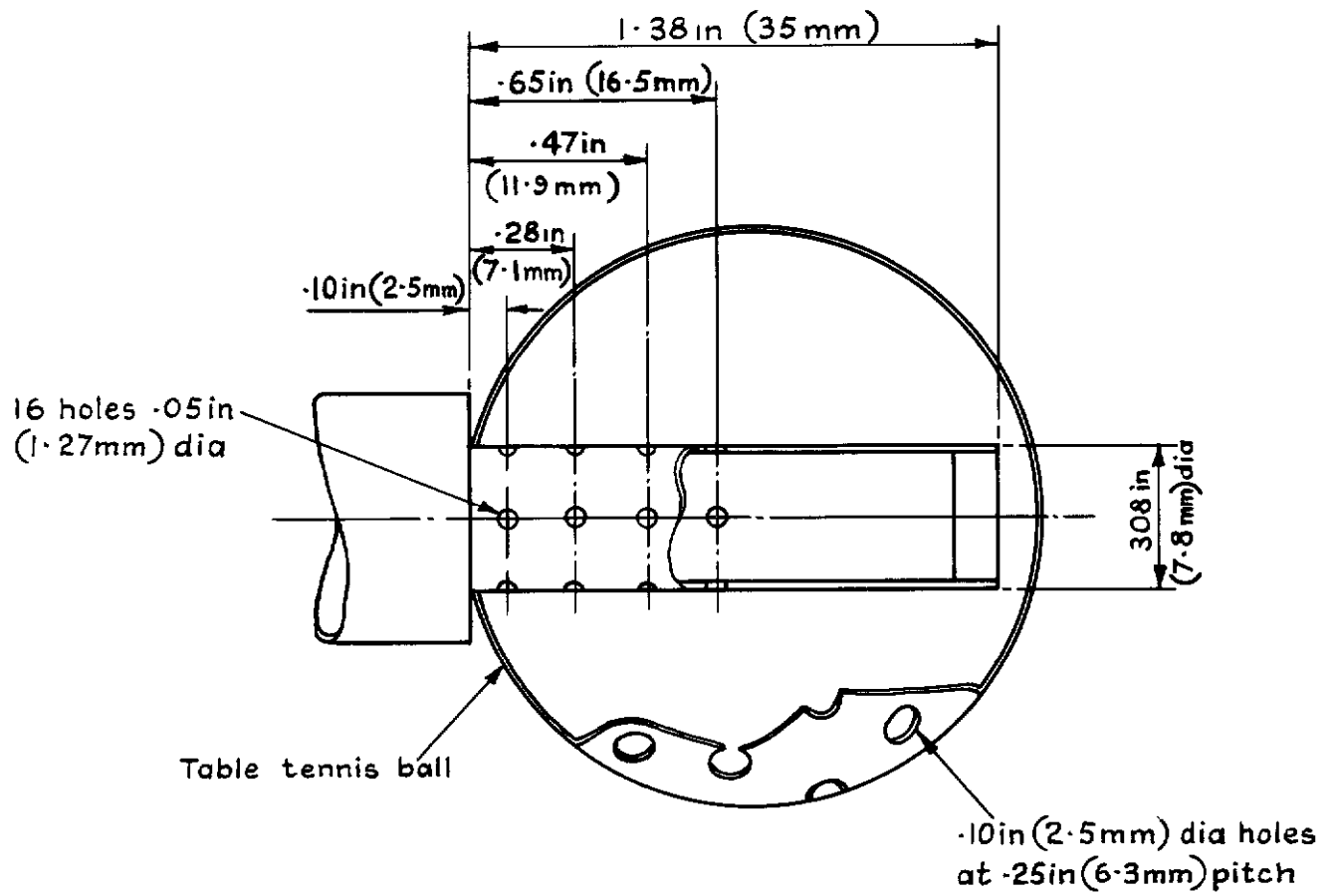


Fig. 3 The perforated sphere static

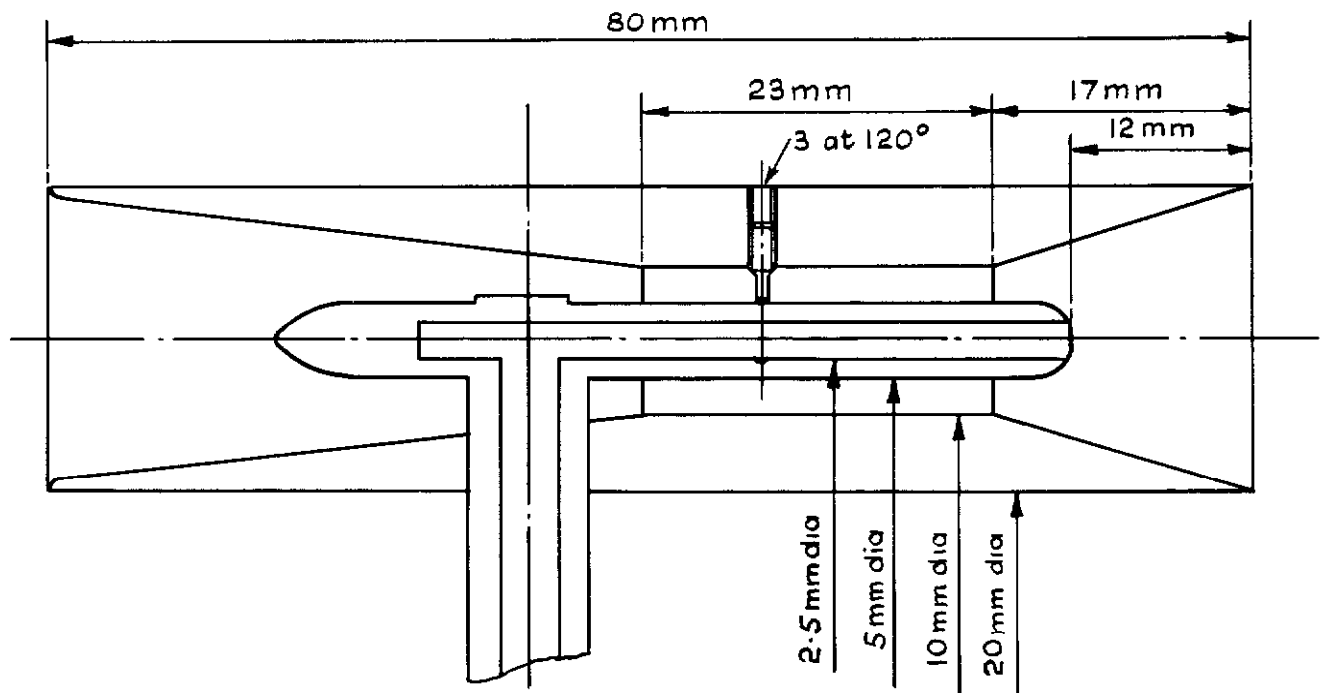


Fig. 4 The venturi pitot

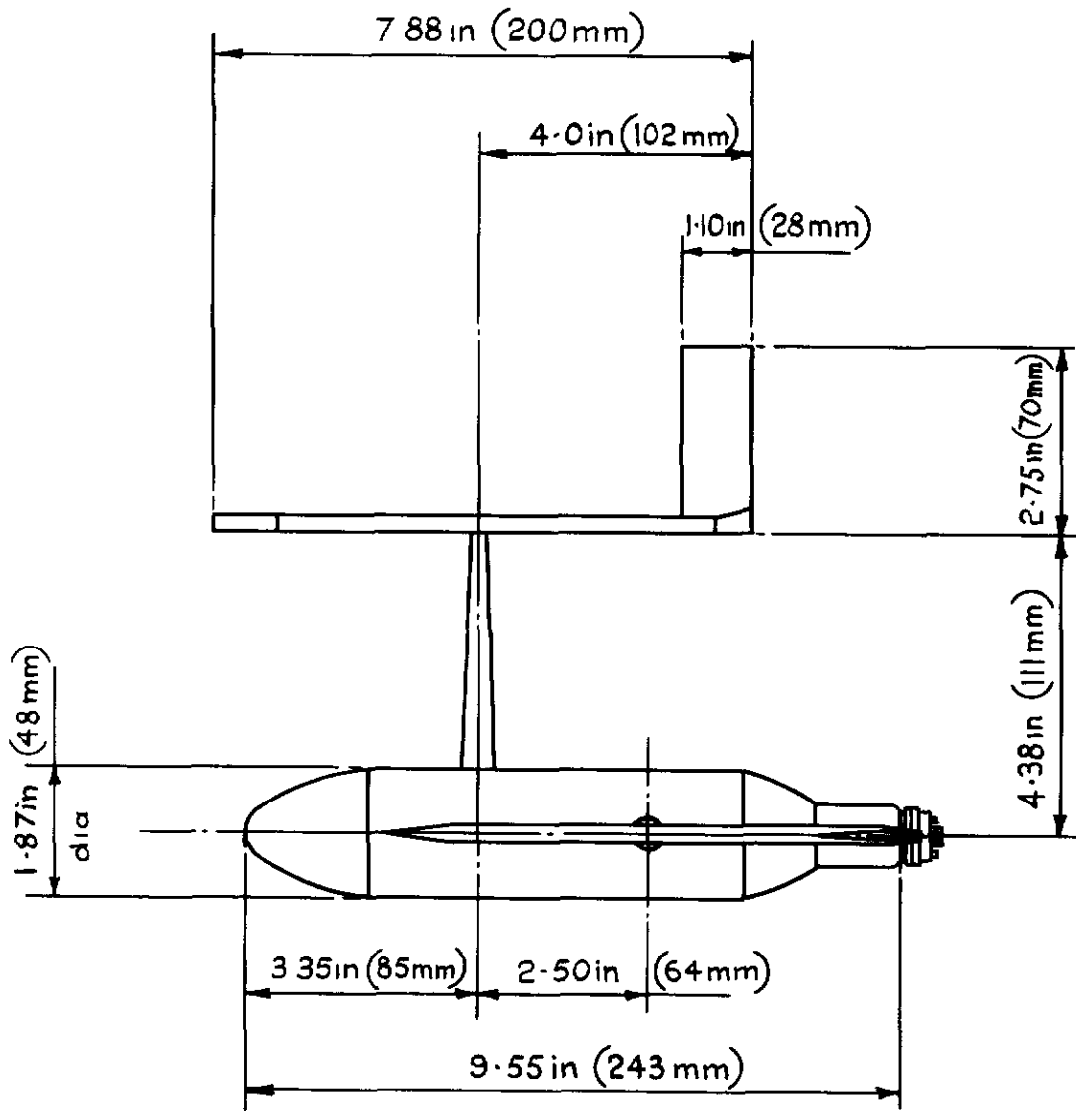


Fig.5 Side view of wind vane assembly

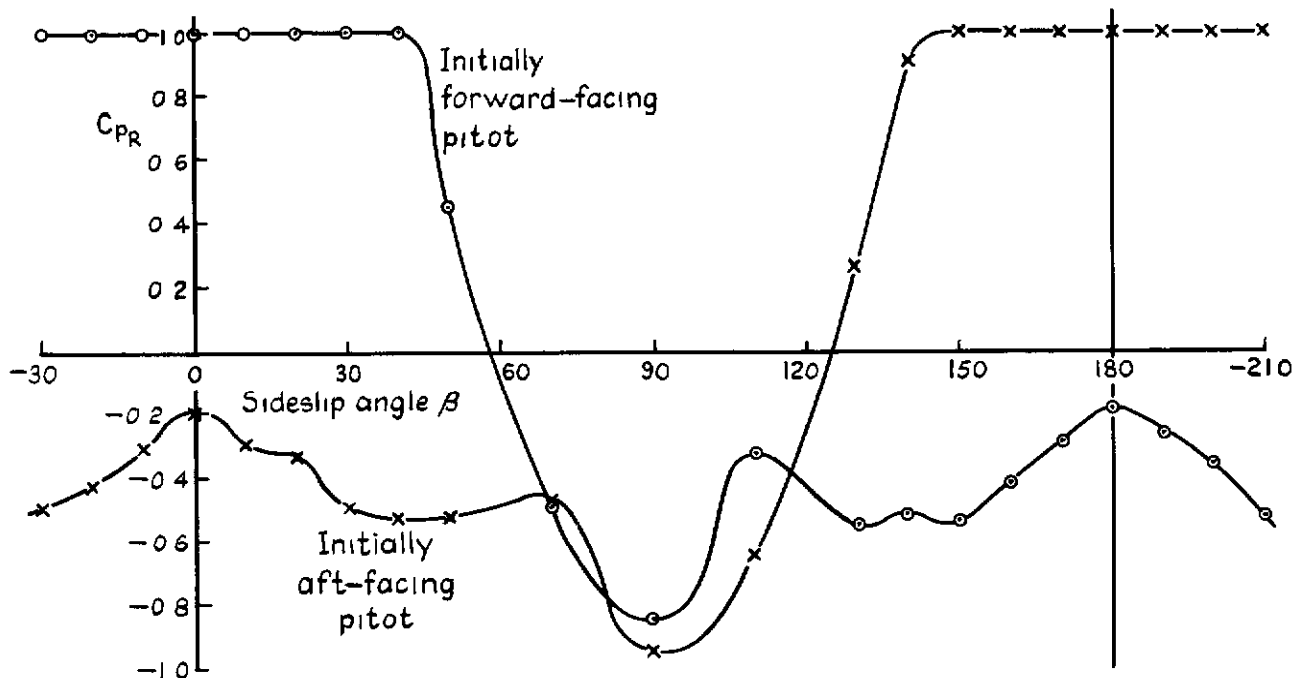


Fig. 6 Variation with sideslip angle of pressures sensed by the two venturi pitots

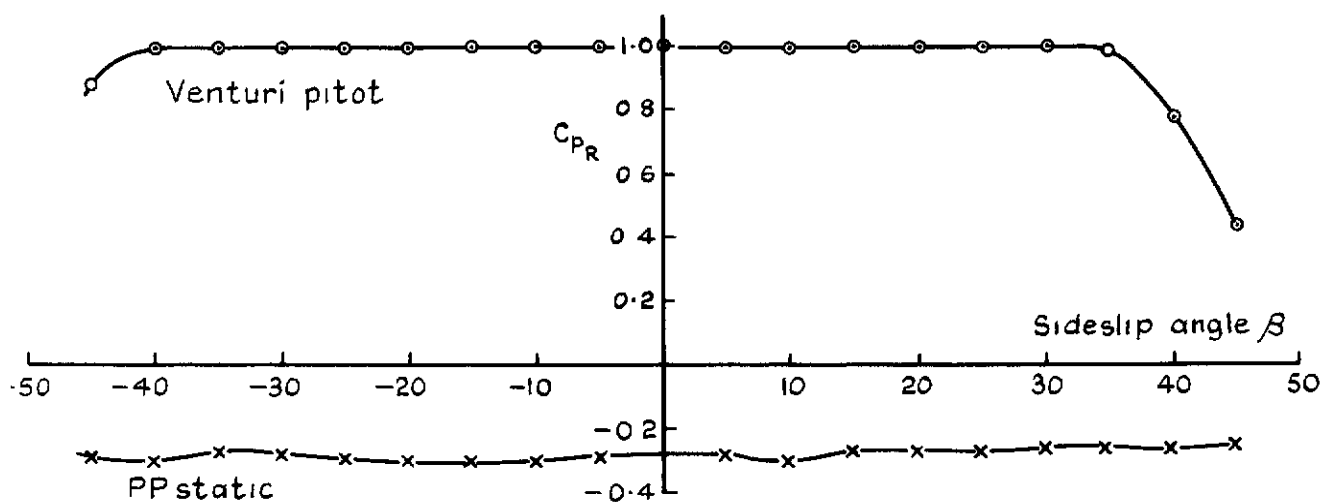


Fig. 7 Variation with sideslip angle of pressures sensed by venturi pitot and PP static

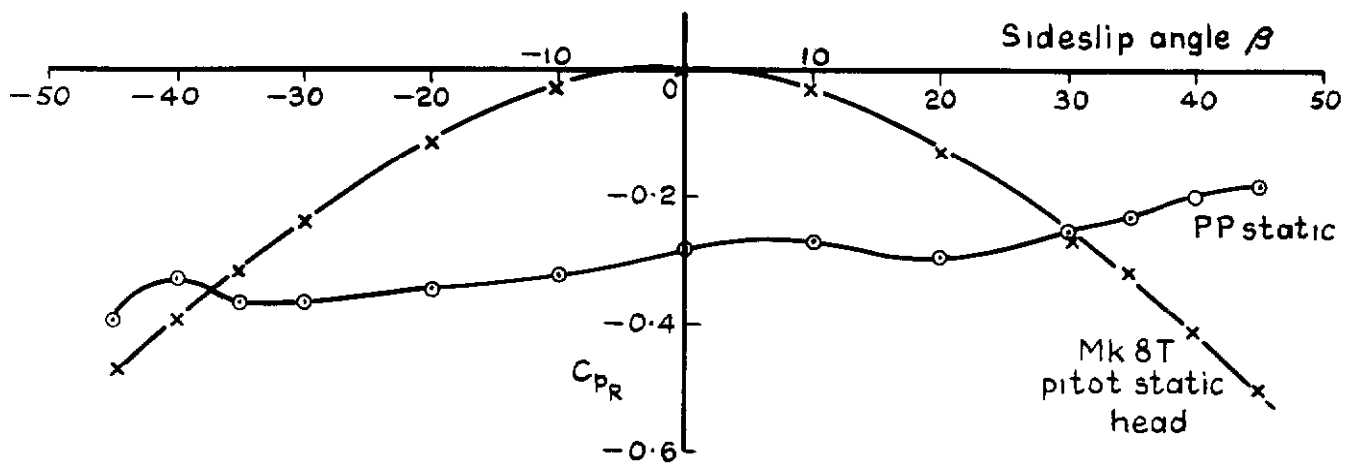


Fig.8 Variation of static pressure with sideslip angle

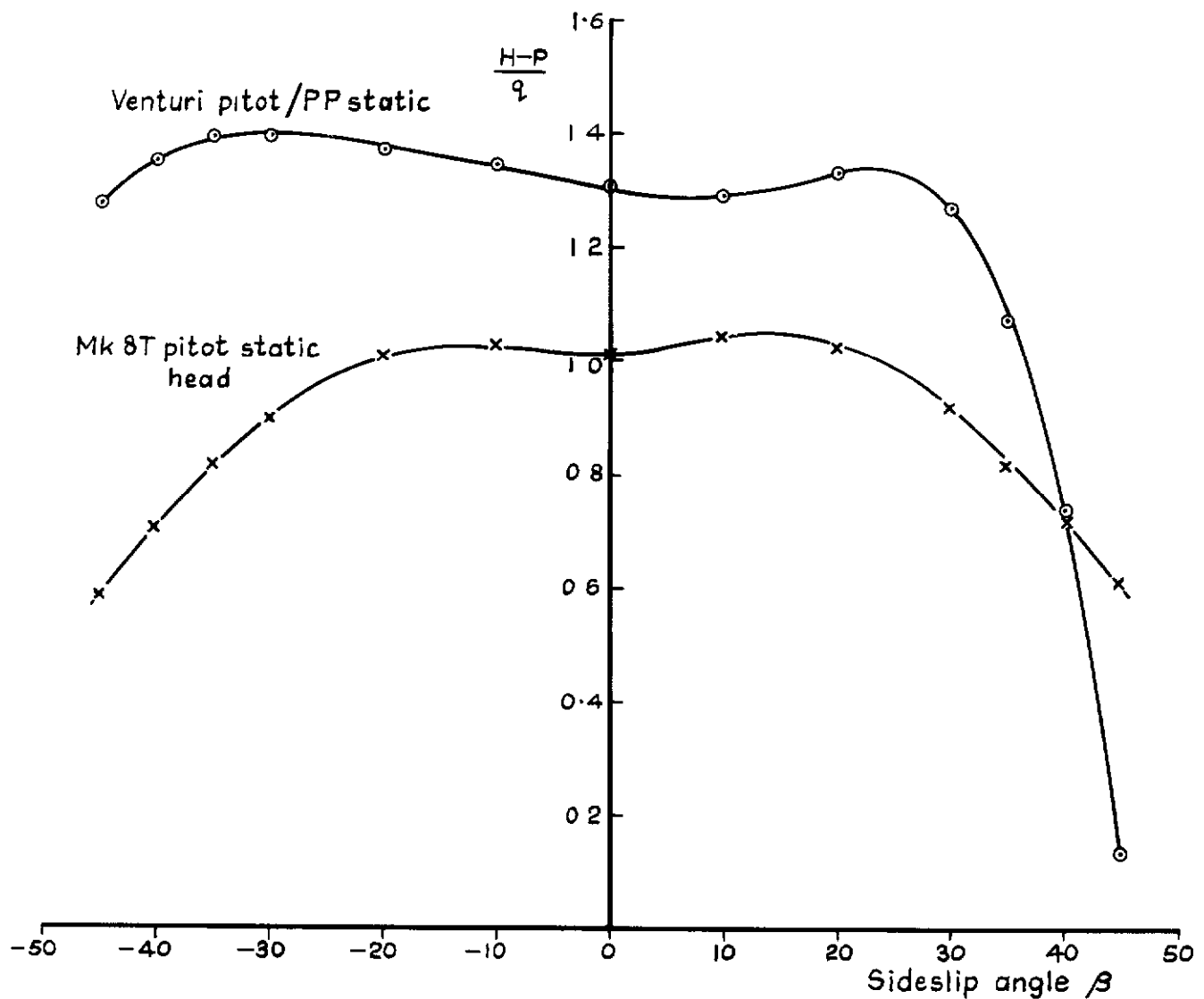


Fig.9 Variation of dynamic pressure with sideslip angle

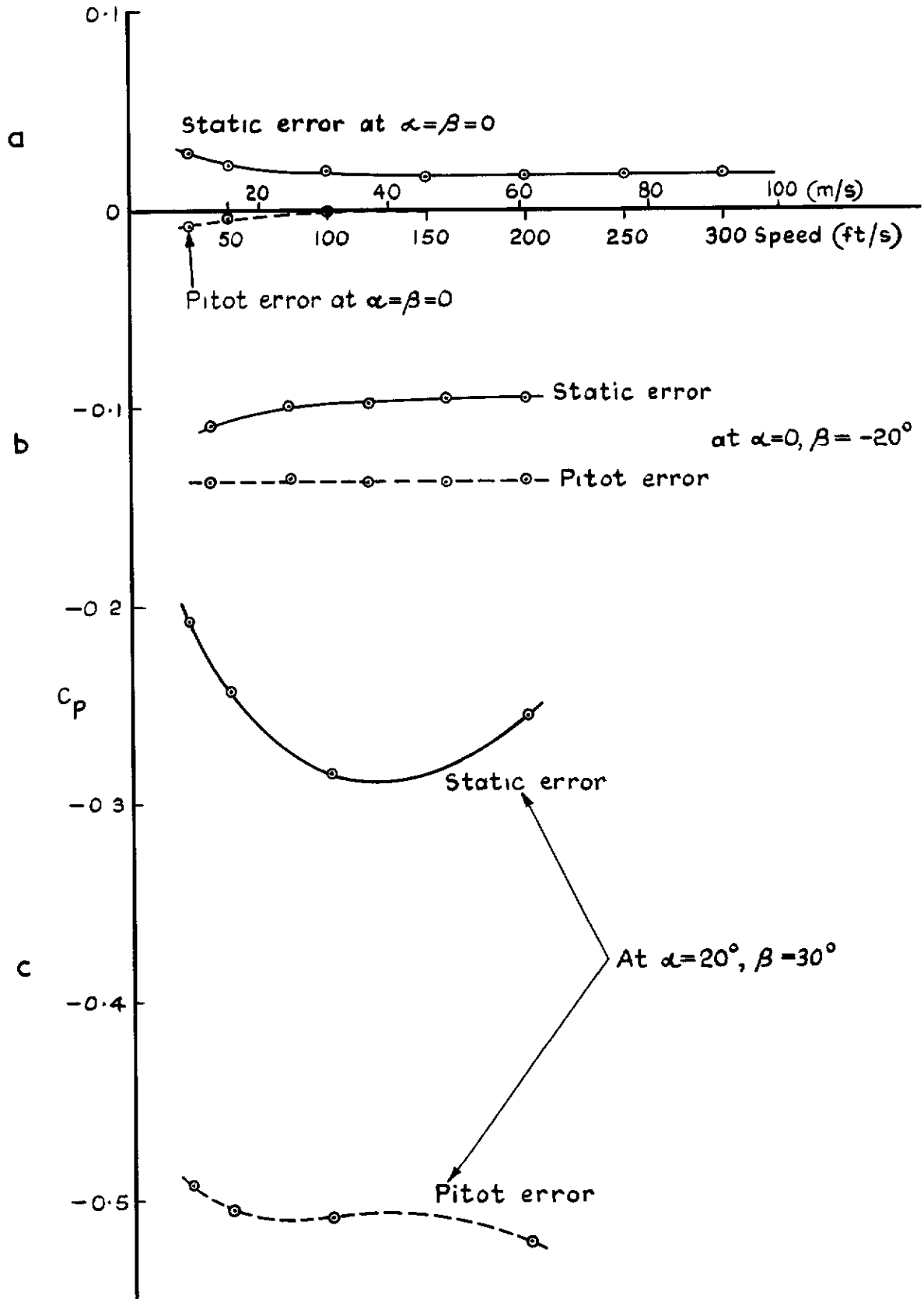
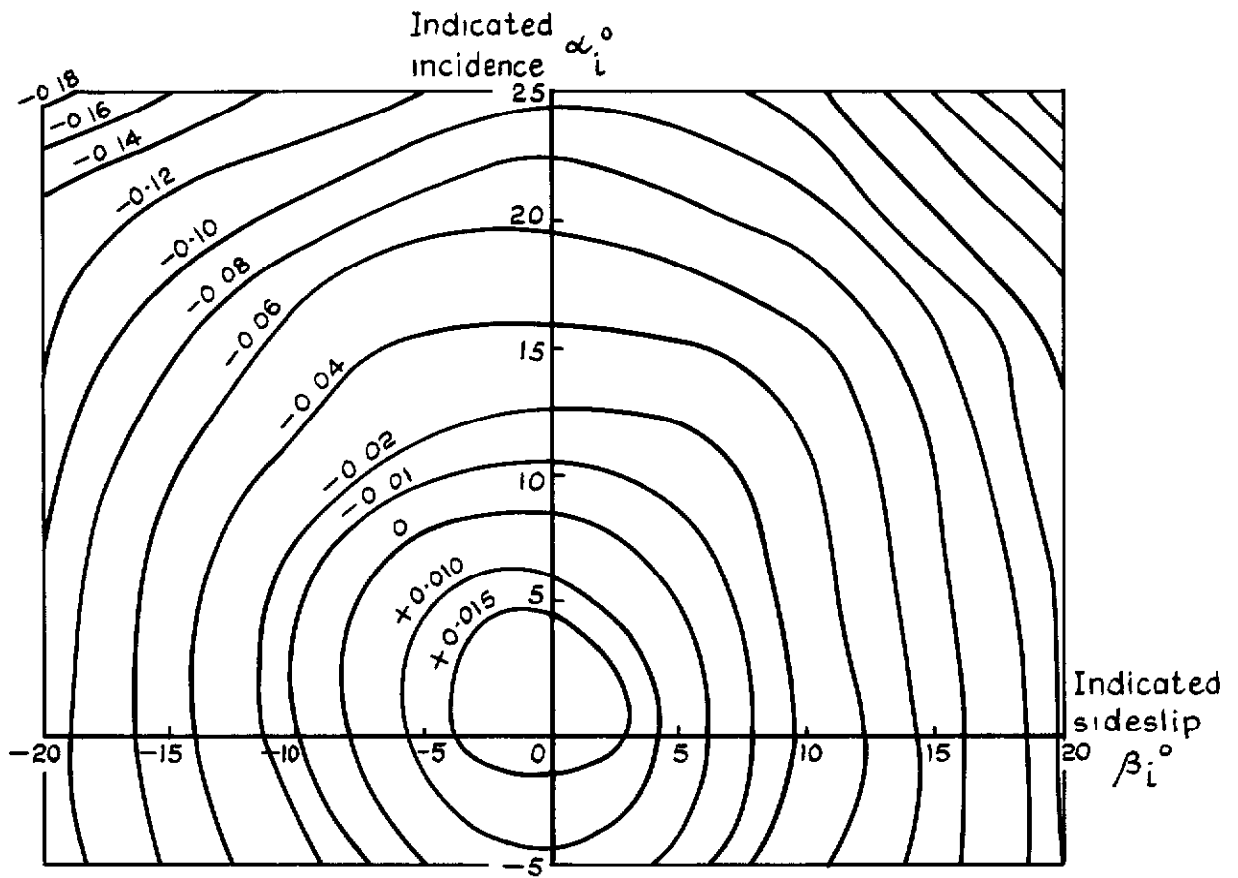
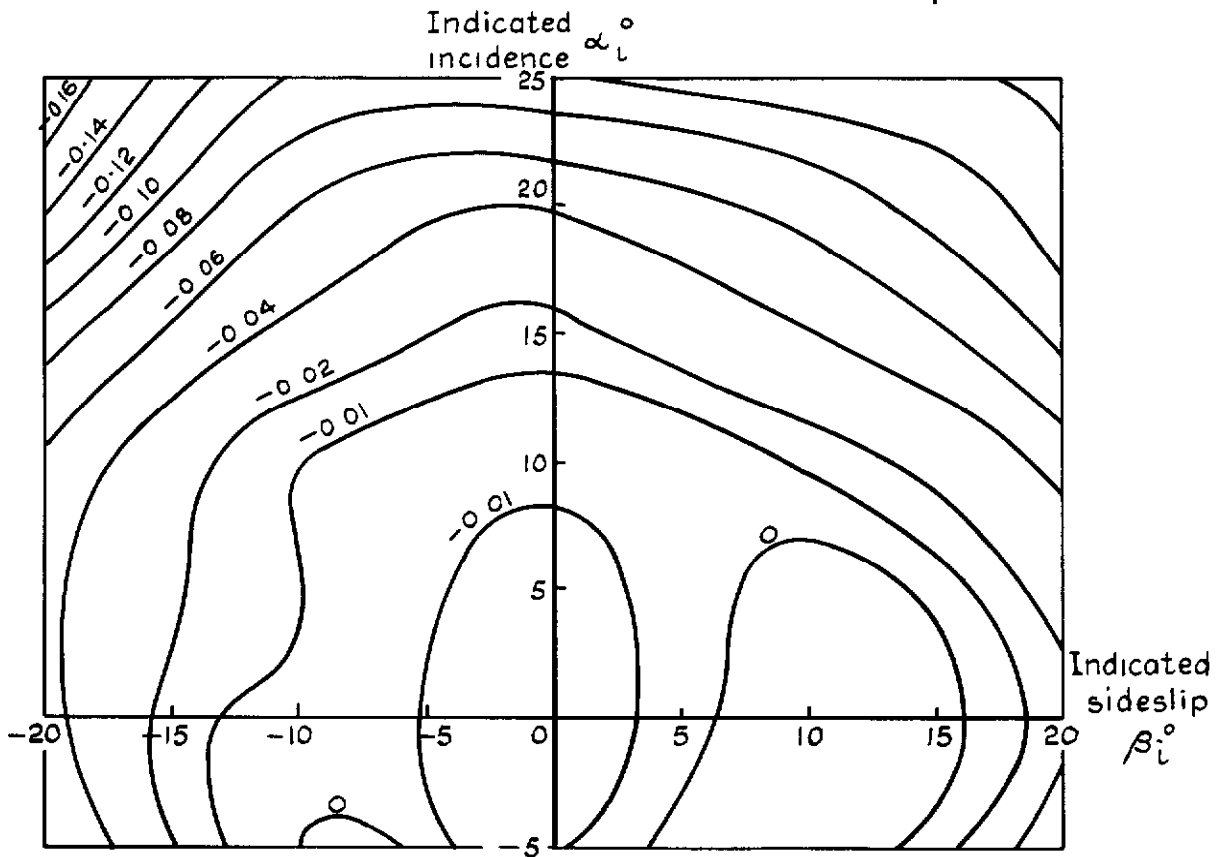


Fig. 10 a-c Variation of pitot and static errors with speed for the Mk 8T pitot static head

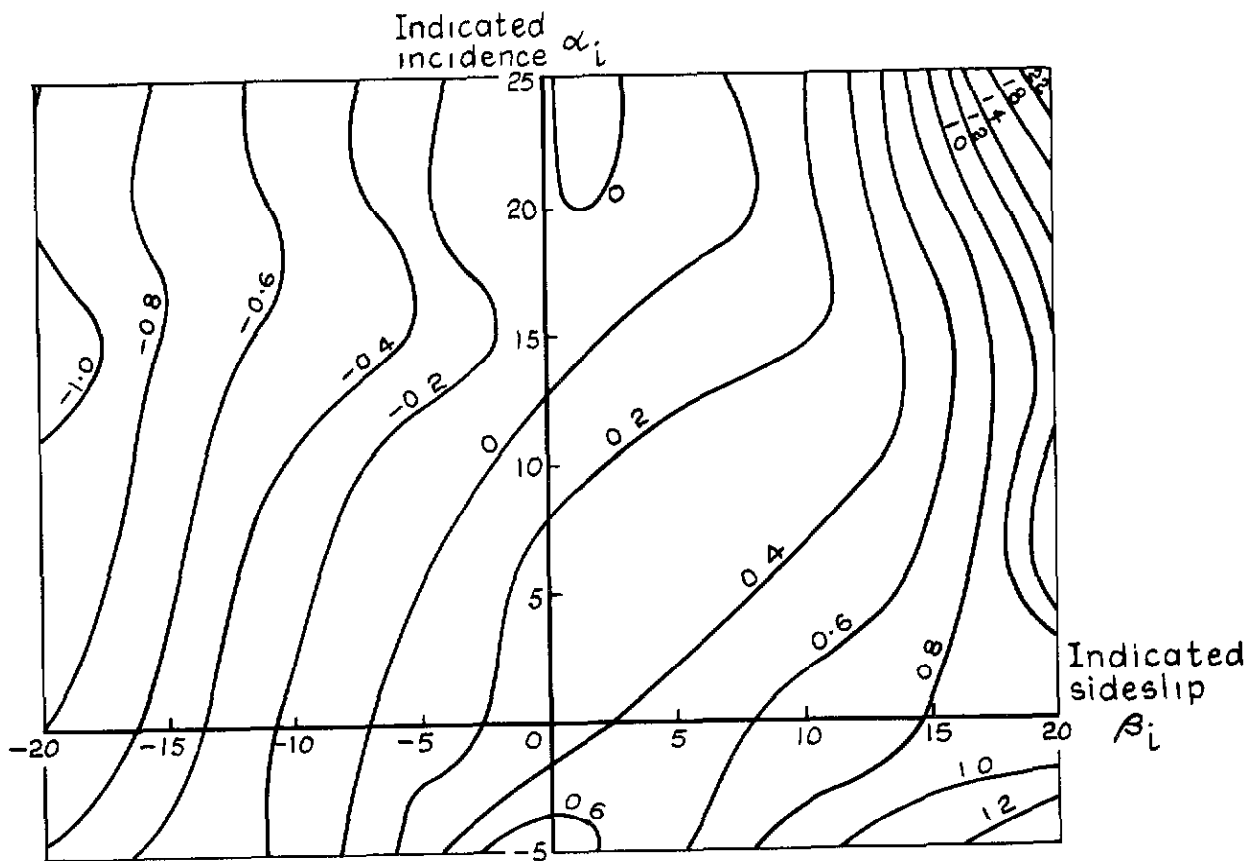


a Static pressure errors. Contours of C_{pP}

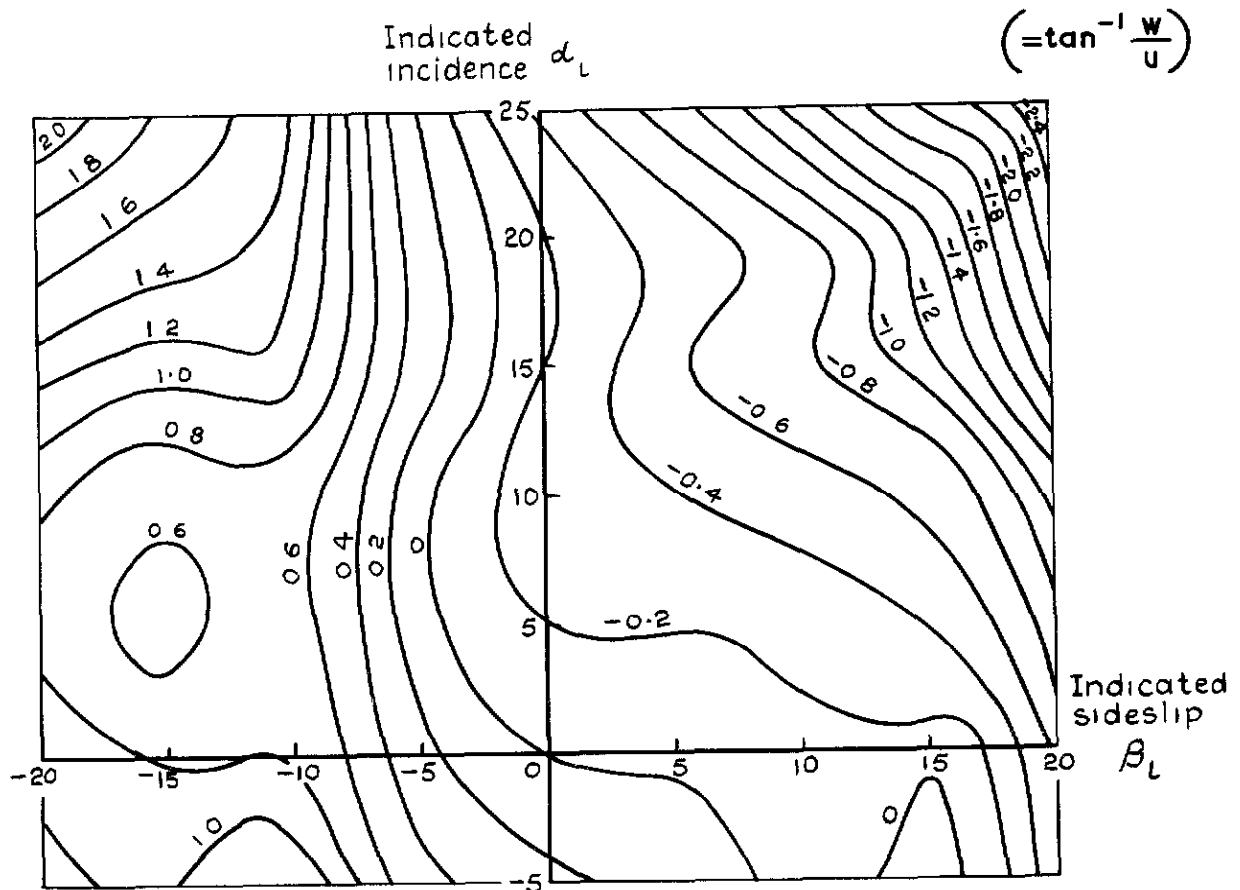


b Dynamic pressure errors. Contours of C_{pD}

Fig.11 a & b Variation of static and dynamic pressure errors with indicated incidence and sideslip for the Mk8T pitot static head



a Incidence vane error corrections. Contours of $\Delta\alpha$ (deg). $\alpha_{\text{true}} = \alpha_i + \Delta\alpha$



b Sideslip vane error corrections. Contours of $\Delta\beta$ (deg). $\beta_{\text{true}} = \beta_i + \Delta\beta$
 $(= \sin^{-1} \frac{v}{V})$

Fig.12 a & b Variation of incidence and sideslip vane error corrections with indicated incidence and sideslip

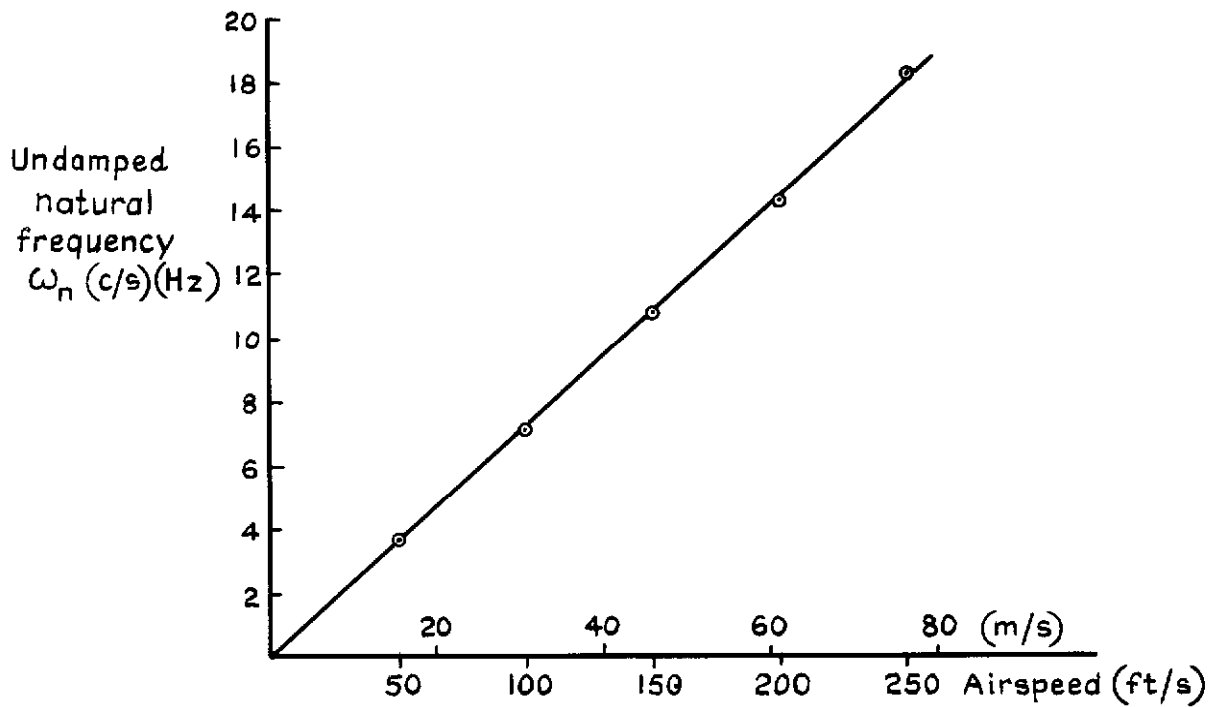


Fig.13 Variation of wind vane natural frequency with airspeed

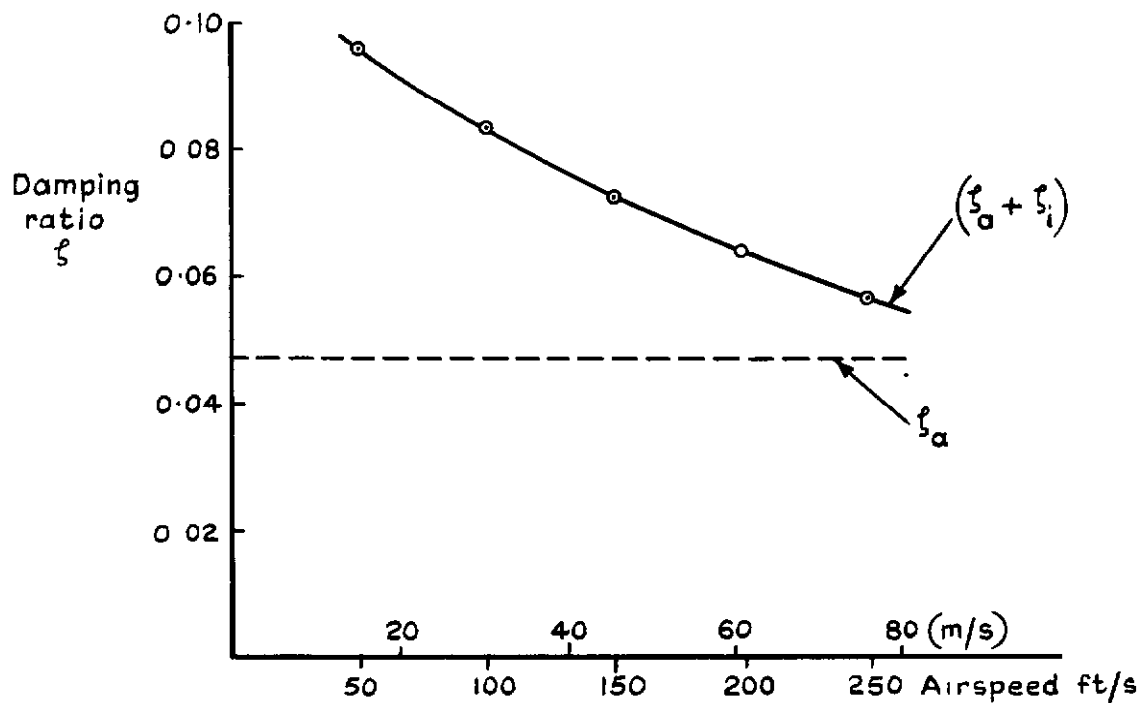


Fig. 14 Variation of wind vane damping ratio with airspeed

DETACHABLE ABSTRACT CARD

A.R.C. C.P No.1162
July 1970

531.7.089.6
533.6.082.32 :
551.508.51

King, K. P
Rowthorn, E. N.

LOW-SPEED WIND-TUNNEL CALIBRATIONS OF THE PITOT AND STATIC PRESSURE SENSORS AND WIND VANES ON THE SHORT SC 1 AIRCRAFT

The pressure sensors tested consisted of a perforated sphere static, a twin venturi pitot arrangement, designed to permit the derivation of dynamic pressure in both forward and backward flight, and a Mk.8T pitot-static head. It was found that only the Mk 8T pitot-static head gave satisfactory results over the range of sideslip angles likely to be met in flight. This pitot-static head was then calibrated over a range of incidence and sideslip angles and error contours were plotted to facilitate the correction of the indicated static and dynamic pressures recorded in flight. The wind vanes measuring sideslip and incidence were also calibrated over the same range and error contours plotted for the correction of their indications. Finally the dynamic response of the wind vanes was investigated to determine their natural frequency and damping and hence their amplitude ratio and phase lag when recording aircraft oscillations.

A.R.C. C.P No.1162
July 1970

531.7 089.6
533 6 082.32
551 508 51

King, K. P
Rowthorn, E. N.

LOW-SPEED WIND-TUNNEL CALIBRATIONS OF THE PITOT AND STATIC PRESSURE SENSORS AND WIND VANES ON THE SHORT SC 1 AIRCRAFT

The pressure sensors tested consisted of a perforated sphere static, a twin venturi pitot arrangement, designed to permit the derivation of dynamic pressure in both forward and backward flight, and a Mk 8T pitot-static head. It was found that only the Mk 8T pitot-static head gave satisfactory results over the range of sideslip angles likely to be met in flight. This pitot-static head was then calibrated over a range of incidence and sideslip angles and error contours were plotted to facilitate the correction of the indicated static and dynamic pressures recorded in flight. The wind vanes measuring sideslip and incidence were also calibrated over the same range and error contours plotted for the correction of their indications. Finally the dynamic response of the wind vanes was investigated to determine their natural frequency and damping and hence their amplitude ratio and phase lag when recording aircraft oscillations.

The pressure sensors tested consisted of a perforated sphere static, a twin venturi pitot arrangement, designed to permit the derivation of dynamic pressure in both forward and backward flight, and a Mk 8T pitot-static head. It was found that only the Mk 8T pitot-static head gave satisfactory results over the range of sideslip angles likely to be met in flight. This pitot-static head was then calibrated over a range of incidence and sideslip angles and error contours were plotted to facilitate the correction of the indicated static and dynamic pressures recorded in flight. The wind vanes measuring sideslip and incidence were also calibrated over the same range and error contours plotted for the correction of their indications. Finally the dynamic response of the wind vanes was investigated to determine their natural frequency and damping and hence their amplitude ratio and phase lag when recording aircraft oscillations.

LOW-SPEED WIND-TUNNEL CALIBRATIONS OF THE PITOT AND STATIC PRESSURE SENSORS AND WIND VANES ON THE SHORT SC 1 AIRCRAFT

King, K. P.
Rowthorn, E. N.

A.R.C. C.P. No.1162
July 1970

531.7.089.6 :
533.6.082.32
551.508.51

C.P. No. 1162

© *Crown copyright 1971*

Published by
HER MAJESTY'S STATIONERY OFFICE

To be purchased from
49 High Holborn, London WC1 V 6HB
13a Castle Street, Edinburgh EH2 3AR
109 St Mary Street, Cardiff CF1 1JW
Brazenose Street, Manchester M60 8AS
50 Fairfax Street, Bristol BS1 3DE
258 Broad Street, Birmingham B1 2HE
80 Chichester Street, Belfast BT1 4JY
or through booksellers

C.P. No. 1162

SBN 11 470430 9